

# The Circulating Balls Heat Exchanger (CIBEX)

Nahum Gat\*

TRW Space and Technology Group, Redondo Beach, California

The CIBEX heat exchanger consists of a gas cooling section (gas generator) and an air heating section (air preheater) coupled with a stream of solid particles. The stream of particles falls through a hot gas stream, picking up heat and cooling the gas, then through the airstream, heating the latter. The cooled particles are then returned to the top of the device and the heating/cooling cycle repeated. The paper describes the two-phase equations of motion for the flow of the spherical particles through the fluid. The solid phase is treated as a pseudo-gas by using concentrations instead of density. The equations are then non-dimensionalized and solved by numerical integration. The solution gives temperature and velocity profiles for the two phases for parametric variations in the solid loading and the fluid flux rate. The solution is applied for the design of a heat exchanger for a hypothetical 2500 tons/day coal gasification plant. The dimensions of the CIBEX heat exchanger are much smaller than those of a comparable conventional heat exchanger.

## Nomenclature

$A$	= flow cross-sectional area
$A, B, C, D, E, F$	= variables, defined in Table 5
$C_D$	= drag coefficient
$C_{pg}$	= specific heat of gas
$C_{pp}$	= specific heat of particle
$d_p$	= particle diameter
$g$	= gravitational acceleration
$h$	= heat-transfer coefficient (combined convective and radiative effects)
$H$	= enthalpy
$k_g$	= gas thermal conductivity
$k_p$	= particle thermal conductivity
$L$	= heat exchanger length
$\dot{m}_g$	= gas flow rate
$\dot{m}_p$	= particle flow rate
$n_p$	= particle number density
$p$	= pressure
$Q_w$	= heat loss to wall
$R$	= gas constant
$S$	= quantity defined in Table 3
$T$	= temperature
$U$	= velocity
$x$	= longitudinal coordinate
$\alpha$	= $0 < \alpha < 1$ defines the fraction of sensible heat loss to the wall
$\Delta$	= defined in Eq. (26), Table 6
$\gamma$	= specific heat ratio for gas
$\epsilon$	= volume fraction of solids
$\eta$	= loading factor
$\mu$	= viscosity
$\rho$	= density
$\sigma$	= concentration
$\bar{\tau}$	= dissipation tensor

## Superscripts

( )<sup>\*</sup> = dimensional quantity

( $\vec{\quad}$ ) = vector quantity  
( )' = derivative with respect to  $x$

## Subscripts

$g$	= gas
$i$	= inlet
$m$	= mean
$p$	= particle
$w$	= wall
0	= at $x=0$ bottom of heat exchanger
1	= at $x=1$ top of heat exchanger

## Introduction

THIS paper describes a concept of a direct-contact heat exchanger/regenerator in which one medium (gas) flows through a moving bed of a second medium (solid particles) and exchanges heat with it. The concept may be utilized for regenerative heat transfer between the high-temperature combustion gas stream and the cold combustion air of a combustor for a magnetohydrodynamic (MHD) generator<sup>1</sup> or for enhancing chemical reactions between a flowing gas stream and a solid material in the metallurgical, chemical, or petroleum industries.<sup>2,3</sup> Schematically shown in Fig. 1, the solid particles fall through a counterflowing hot gas stream in the gas generator. The gas cools by heat transfer to the particles. The particles then fall through the air preheater in which they give off heat to the combustion air. The particles are then recirculated back into the gas generator via a pneumatic or mechanical lift. The concept is of interest because of its high potential to provide relatively maintenance-free heat exchange in a compact package and is particularly suitable for a stream of dirty combustion products such as in coal combustors and gasifiers. In addition, such a heat exchanger is smaller in size than similarly rated conventional heat exchangers and provides greater heat recovery, low-pressure drop, and easy access for cleaning.

## Mathematical Formulation

The two-phase counterflow in the heat exchanger can be described by writing the conservation equations (mass, momentum, and energy) for each phase separately, including the terms for interaction between the phases.<sup>4</sup> In theory, the gas flows in the open spaces between the particles. As the number density of the particles changes, so does the available

Received April 14, 1986; presented as Paper 86-1304 at the AIAA/ASME 4th Thermophysics and Heat Transfer Conference, Boston, MA, June 2-4, 1986; revision received Aug. 8, 1986. Copyright © American Institute of Aeronautics and Astronautics, Inc., 1987. All rights reserved.

\*Combustion and Experiments Section Manager, Applied Technology Division.

cross-sectional area for the gas flow. To avoid the issue of dealing with a variable-area flow, the problem is formulated in terms of concentrations rather than densities. Several definitions, listed in Table 1, are helpful. With these definitions, the stream of particles is treated here as a pseudo-gas, or a continuum, having a "density" specified by its concentration. The following is a list of assumptions underlying the analysis:

- 1) Steady one-dimensional flow.
- 2) Particles are uniformly distributed over each cross section.
- 3) Particles are spherical and of a uniform size.
- 4) The volume occupied by the particles cannot be neglected.
- 5) Particles are spread far enough so that the motion of each one is unaffected by the motion of its neighbors or by the wake of the preceding particles.
- 6) The particles are large enough and no random motion (Brownian-type motion) exists. The pressure in the mixture is that of the gas.
- 7) Particles do not interact with the boundaries and in the case of uniform size distribution, particles do not interact with each other.
- 8) The boundary-layer effect on the flow is neglected.
- 9) Gas is perfect and compressible and its physical properties are a function of temperature only.
- 10) The temperature of each particle is uniform with no internal gradients.
- 11) Radiative exchange between the balls and the boundaries or among the balls is neglected.

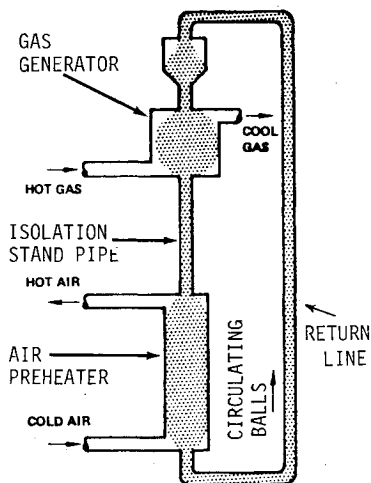


Fig. 1 The CIBEX concept.

These assumptions are meant to simplify the mathematical formulation, but are not quite always met. The corrections for the nonideal effects can be estimated and shown to be small. Assumption 2 depends on the mechanical design of the balls' distribution system. Assumption 5 allows a simple treatment of the drag laws. In reality, the drag is modified by the proximity of the particles. Once a different drag force model is selected, it may be substituted into the model. Assumption 7 also depends on the mechanical design and the actual drag force acting on the balls. Assumption 10 indicates a small Biot number (i.e., the internal heat transfer is higher compared with the heat transfer between the solid and gas phases). In assumption 11, the radiative exchange between the balls and the wall may be neglected since the wall is hot. Radiative exchange among the particles, however, may cause a deterioration in performance. For the conditions described in this paper, the balls' number density is between 2-4 balls/cm<sup>3</sup>, which make the optical depth for extinction less than 50-25 cm, respectively. The resulting small effect of longitudinal radiative diffusivity can be added to the model.

#### Equations of Motion

The equations of motion are listed in Table 2 for the gas and solid phases. In Eq. (3), the change in momentum is attributed to the body forces acting upon the pseudo-gas phase. The second term on the right-hand side is the drag force per unit volume. In Eq. (5), it is assumed that the change in the energy of the particles occurs solely due to heat exchange with the environment. The heat transfer coefficient  $h^*$  may be composed of both convective and radiative terms. Presently, only the convective term is taken into account.

In Eq. (6),  $\dot{Q}_w^*$  is the rate of heat loss to the walls

$$\dot{Q}_w^* = \rho_{gi}^* C_{pgi}^* T_g^* \frac{U_{gi}^*}{L^*} \alpha$$

and  $\alpha$  designates the fraction loss. Other terms in the gas equation stand for the pressure work, thermal conductivity, viscous dissipation, and heat exchange with the particles.

#### Equation of State

It can be shown that the pressure in the system is composed of the partial pressures of the two phases. For a mixture in thermal equilibrium,

$$p^* = \sigma_m^* R^* T^*$$

Table 1 Basic definitions of two-phase flow quantities

Quantity	Definition	Units
Number density of particles	$n_p^* = \frac{\dot{m}_p^*/A^*}{\rho_p^* (\pi d_p^{*3}/6) U_p^*}$	Particles/volume
Volume fraction occupied by the particles	$\epsilon = n_p^* \frac{\pi d_p^{*3}}{6}$	Dimensionless
Volume fraction occupied by the gas	$1 - \epsilon$	Dimensionless
Gas concentration	$\sigma_g^* = \rho_g^* (1 - \epsilon)$	Weight/volume
Particles concentration	$\sigma_p^* = \rho_p^* \epsilon$	Weight/volume
Loading ratio	$\eta = \frac{\dot{m}_p^*}{\dot{m}_g^*} = \frac{\sigma_p^* U_p^*}{\sigma_g^* U_g^*}$	Dimensionless

Table 2 Equation of motion for the two-phase flow

Solid phase		Gas phase	
Continuity	$\sigma_p^* u_p^* A^* = \dot{m}_p^*$ (1)	Continuity	$\sigma_g^* u_g^* A^* = \dot{m}_g^*$ (2)
Momentum	$\sigma_p^* \frac{DU_p^*}{Dt^*} = \sigma_p^* \bar{g}^* - \frac{\sigma_g^*}{2} (\bar{U}_p^* - \bar{U}_g^*)  \bar{U}_p^* - \bar{U}_g^*  C_{Dp} A_p^* n_p^*$ (3)	Momentum	$\sigma_g^* \frac{D\bar{U}_g^*}{Dt^*} = -\nabla p^* + \nabla \cdot \bar{\tau} + \frac{\sigma_g^*}{2} (\bar{U}_p^* - \bar{U}_g^*)  \bar{U}_p^* - \bar{U}_g^*  C_{Dp} A_p^* n_p^*$ (4)
Energy	$\sigma_p^* \frac{DH_p^*}{Dt^*} = -h^* A_s^* n_p^* (T_p^* - T_g^*)$ (5)	Energy	$\sigma_g^* \frac{DH_g^*}{Dt^*} = U_g^* \frac{dp^*}{dx^*} + h^* A_s^* n_p^* (T_p^* - T_g^*) + \dot{Q}_w^* + k_g^* \frac{d^2 T_g^*}{dx^{*2}} + \frac{4}{3} \mu_g^* \left( \frac{dU_g^*}{dx^*} \right)^2$ (6)
State	$\rho_p^* = \text{const}$ (7)	State	$p^* = \sigma_g^* R^* T_g^*$ (8)
Transport properties	$C_{pp}^* = \text{const}$ (9)	Transport properties	$\frac{C_{pg}^*}{R^*} = 4.7692 - \frac{970.85}{T_g^*} + \frac{1.803 \times 10^5}{T_g^{*2}}$ (10)
			$\mu_g^* = 1.78 \times 10^{-5} \left( \frac{T_g^*}{300} \right)^{0.5} \left[ \frac{\text{kg}}{\text{m} \cdot \text{s}} \right]$ (11)
			$k_g^* = 4.982 \times 10^{-2} + 5.164 \times 10^{-5} (T_g^* - 700) \left[ \frac{\text{W}}{\text{m} \cdot \text{K}} \right]$ (12)

where

$$\sigma_m^* = \sigma_g^* + \sigma_p^* = (1 - \epsilon) \rho_g^* + \epsilon \rho_p^*$$

Thus, for a mixture in which the partial volume of solids is small ( $\epsilon \ll 1$ ), the partial pressure of the solids may be neglected and the equation of state for the gas and solid phases are given on Table 2.

**Transport Properties**

For simplicity, it is assumed that the specific heat of the solid phase is constant. For the gas, the dependence of the transport properties on the temperature is given in Table 2. The specific heat (e.g., Eq. 10) is that of  $N_2$  after units conversion of the data in Ref. 5. The viscosity and thermal conductivity are obtained by linear regression of the data in Ref. 6.

In summary, the number of unknowns is seven ( $\rho_g^*, T_g^*, P_g^*, P_p^*, U_g^*, U_p^*, \epsilon$ ), same as the number of equations [(Eqs.1-8)].

**Coordinate System**

The positive  $x$  direction is chosen in the upward direction and the velocity vector can be expressed in terms of the scalar speed as  $\bar{U}_p = U_p \vec{x}$  and  $\bar{U}_g = U_g \vec{x}$ . Similarly, the following relationships are useful:  $dx_p = U_p dt$ ,  $dx_g = U_g dt$ , and  $\vec{g} = -\vec{g}x$ .

**Nondimensional Equations**

The following terms are used to nondimensionalize the equations:

$$x = \frac{x^*}{L^*}, \quad \sigma = \frac{\sigma^*}{\rho_{gi}^*}, \quad U = \frac{U^*}{U_{gi}^*}, \quad T = \frac{T^*}{T_{gi}^*}$$

$$\mu_g = \frac{\mu_g^*}{\mu_{gi}^*}, \quad k_g = \frac{k_g^*}{k_{gi}^*}, \quad C_{pg} = \frac{C_{pg}^*}{C_{pgi}^*}$$

Next, to reduce the number of equations and variables, the two continuity equations are substituted into the correspond-

ing momentum and energy equations. Similarly, the equation of state is substituted into the momentum and energy equations. Using the coordinate system and the dimensionless parameters, and after some rearrangement, the four equations with four unknowns  $T_g, U_g, T_p,$  and  $U_p$  can be written as shown in Table 3. The table also gives the definition of the dimensionless numbers appearing in the problem. Finally, the drag coefficient, heat-transfer coefficient, and additional quantities calculated at the local conditions are given in Table 4. The correlations for the drag coefficients have been derived in Ref. 7 to fit the experimental data of Ref. 8. The heat-transfer coefficient is expressed by the Nusselt number according to the Ranz-Marshall correlation.

**Boundary Conditions**

The boundary conditions are specified for the gas at the bottom (i.e., at  $x = 0$ ) and for the particles at the top ( $x = 1$ ) of the heat exchanger. The nondimensional boundary conditions

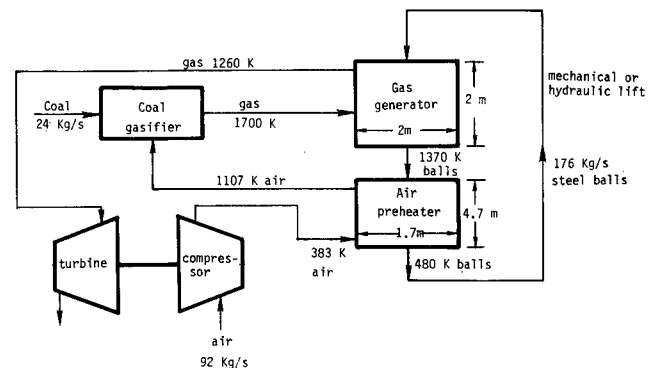


Fig. 2 Approximate sizing of a CIBEX for a 2500 ton/day coal gasification plant operating at 30 atm.

Table 3 Reduced equations of motion and the dimensionless quantities

Momentum				(13)
	$\frac{dU_p}{dx} = -\frac{1}{U_p Fr} + \frac{3}{4} \frac{(U_p + U_g)^2}{U_p U_g} \frac{C_D}{S}$			
	$\frac{dU_g}{dx} = -\frac{1}{\gamma M_i^2} \frac{d}{dx} \left( \frac{T_g}{U_g} \right) - \frac{3}{4} \frac{(U_p + U_g)^2}{U_p U_g} C_D \frac{\eta}{S} - \frac{4}{3 Re(L/d_p)} \frac{d^2 U_g}{dx^2}$			(14)
	$\frac{dT_p}{dx} = 6 \frac{Nu}{Re Pr} k_g C_{pr} \frac{(T_p - T_g)}{Su_p}$			(15)
Energy				
	$\frac{d}{dx} \left[ \left( \frac{C_{pg}^*}{R^*} \right) T_g \right] = U_g \frac{d}{dx} \left[ \frac{T_g}{U_g} \right] + 6 \frac{Nu}{Re Pr} k_g \left( \frac{C_{pgi}^*}{R^*} \right) \frac{\eta}{S} \frac{(T_p - T_g)}{U_p}$			
	$+ \frac{(C_{pgi}^*/R^*)}{Re Pr(L/d)} \frac{d^2 T_g}{dx^2} + \frac{\gamma M_i^2}{Re(L/d)} \left( \frac{dU_g}{dx} \right)^2 - \left( \frac{C_{pg}^*}{R^*} \right) T_g \alpha$			(16)
Dimensionless reference quantities				
Reynolds number	$Re = \frac{\rho_{gi}^* U_{gi}^* d_p^*}{\mu_{gi}^*} = \frac{m_g^*/A^* d_p^*}{\mu_{gi}^*}$		$S = \left( \frac{d_p^*}{L^*} \right) \left( \frac{\rho_p^*}{\rho_{gi}^*} \right)$	
	$Re_p = Re \frac{U_p/U_g + 1}{\mu_g}$			
Prandtl number	$Pr = \frac{\mu_{gi}^* C_{pgi}^*}{k_{gi}^*}$	Mach number	$M_i = \frac{U_{gi}^{*2}}{\gamma R^* T_{gi}^*}$	
Peclet number	$Pe = Re Pr$	Nusselt number	$Nu = h^* \frac{d_p^*}{k_g^*}$	
Froude number	$Fr = \frac{U_{gi}^{*2}}{L^* g^*}$	Stanton number	$St = \frac{Nu}{Re Pr} = \frac{Nu}{Pe}$	

are, therefore,

$$\begin{aligned} \text{at } x=0, T_g = 1 \text{ and } u_g = 1 \\ \text{at } x=1, T_p = T_{p1} \text{ and } u_p = 0 \end{aligned} \quad (17)$$

Here  $T_{p1} = T_{p1}^*/T_{gi}^*$  is the inlet temperature of the solid phase.

### Solution

An order-of-magnitude analysis indicates that the Reynolds number may vary between 5–2500. The heat exchanger dimension  $L^*/d_p^*$  is of the order of 1000–10,000. The quantity  $S$  is 1 to 50 and the Mach number is smaller than 0.001. Accordingly, only meaningful terms are kept in the equations of motion. The second derivative of velocity term is dropped [Eq. (14)] and the thermal conductivity term and the dissipation term in Eq. (16) are dropped, but the pressure work terms are retained [Eqs. (14) and (16)]. By further differentiation and rearrangement, Eqs. (13–16) may be expressed as four equations with four unknowns, which are the following derivatives:  $U'_p$ ,  $U'_g$ ,  $T'_p$ , and  $T'_g$ , (the prime denotes the derivative with respect to the  $x$  coordinate) as shown in Table 5. Finally, to facilitate numerical integration, Eqs. (18–21) can be solved and the four unknowns expressed in terms of the independent variables as shown in Table 6. This formulation is particularly convenient to use in numerical integration once the boundary conditions are specified.

### Results

The set of Eqs. 22–25 has been solved numerically, using the boundary conditions of Eqs. (17). The integration follows the Runge-Kutta technique and it requires a guess of the solution at  $x=1$  so that the integration may proceed from  $x=1$  down to  $x=0$ . If the derived conditions at the bottom ( $x=0$ ) do not match the given boundary conditions, a new guess is made and the integration is repeated. An intelligent new guess can be made on the basis of the results of the integration. This “shooting” technique is repeated until all boundary conditions are matched.

In order to obtain a realistic solution to the problem, the heat exchanger has been matched with a hypothetical coal gasification plant. A block diagram of the complete plant is shown in Fig. 2. The heat exchanger model is solved then to select the optimal dimensions of the gas generator, the air preheater, and the balls' material and size. The parameter variations included the following:

- Pressure: 6 and 30 atm
- Balls' material: stainless steel (density 8330 kg/m<sup>3</sup>,  $C_p = 461$  J/kg·K) and ceramic (density 3717 kg/m<sup>3</sup>,  $C_p = 1047$  J/kg·K)
- Balls' size: 1, 1.6, 2.0 mm
- Loading parameter: 0.8–2.0

Typical results of these calculations are shown in Figs. 3–8.†

†The curves in these figures are drawn between discrete calculated points. Therefore, the sharp flexures have no physical significance.

Table 4 Drag and heat transfer coefficients

Drag coefficient	
$C_D = \frac{24}{Re_p} + 4.5$	for $0 < Re_p < 1$
$\lg C_D = \lg 28.5 - \frac{24}{28.5} \lg Re_p + 0.06919 (\lg Re_p)^2$	for $1 \leq Re < 60$
$\lg C_D = 2.0065 - 1.3830 \lg Re_p + 0.19887 (\lg Re_p)^2$	for $60 \leq Re < 3000$
$C_D = 0.4$	for $Re \geq 3000$
Heat-transfer coefficient	
$Nu = 2 + 0.6 Re_p^{1/2} Pr_p^{1/3}$	
Local viscosity	
	$\mu_g = T_g^{1/2}$
Local Prandtl number	
$Pr_p = Pr \frac{\mu_g C_{pg}}{k_g}$	
Ratio of specific heats between gas and particles	
	$C_{pr} = C_{pgi}^* / C_{pp}^*$

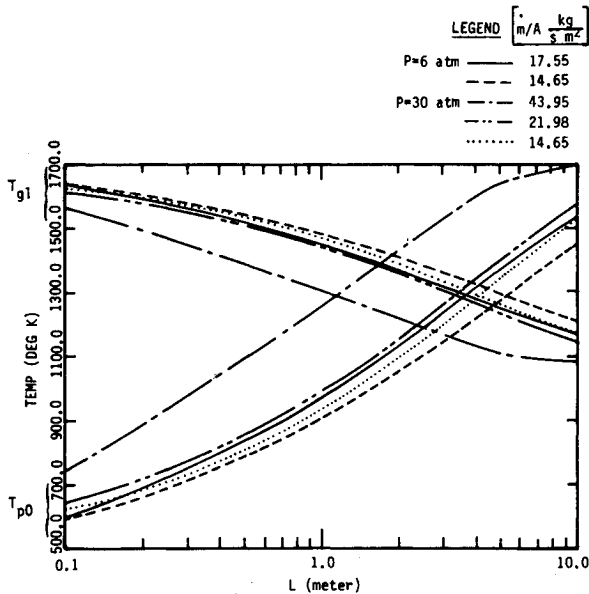


Fig. 3  $T_{g1}$  and  $T_{p0}$  variation with length of gas generator:  $d_p = 1.6$  mm, pressure is 6 and 30 atm, stainless steel balls.

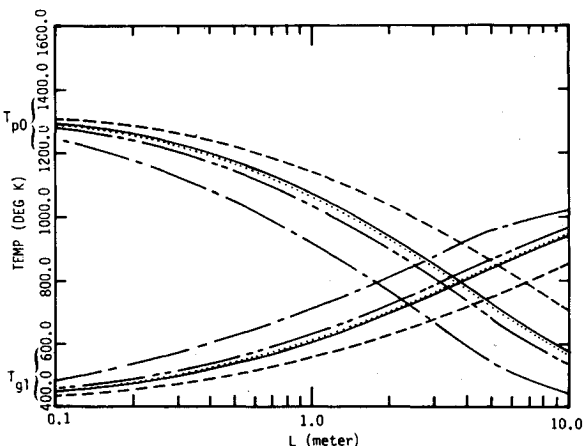


Fig. 4  $T_{g1}$  and  $T_{p0}$  variation with length of air preheater:  $d_p = 1.6$  mm, 6 and 30 atm, stainless steel balls (legend as in Fig. 3).

Table 5 Reduced equations of motion

$$U_p' + 0 + 0 + 0 = -\frac{1}{U_g Fr} + A \frac{C_D}{S} \tag{18}$$

$$0 + BU_g' + CT_g' + 0 = -A \frac{C_D}{S} \eta \tag{19}$$

$$0 + 0 + 0 + T_p' = 6S_t k_g C_{pr} \frac{D}{S} \tag{20}$$

$$0 + FU_g' + ET_g' + 0 = 6S_t k_g \left( \frac{C_{pg}^*}{R^*} \right) \frac{D}{S} \eta - Q \tag{21}$$

where

$$A = \frac{3}{4} \frac{(U_p + U_g)^2}{U_p U_g}$$

$$D = \frac{T_p - T_g}{U_p}$$

$$B = 1 - \frac{T_g}{\gamma M_i^2 U_g^2}$$

$$E = 3.7692 - \frac{1.803 \times 10^5}{T_g^2}$$

$$C = \frac{1}{\gamma M_i^2 U_g}$$

$$F = \frac{T_g}{U_g}$$

$$Q = \alpha \frac{C_{pgi}^*}{R^*} T_g$$

These results have been used for the sizing of the heat exchanger unit in Fig. 2. Figure 3 shows the heat exchange between the gas and stainless steel balls in the gas generator. The figure shows the balls' temperature at the bottom of the gas generator and the gas temperature at the top of the generator for different lengths of generator. Similarly, Fig. 4 shows the balls temperature at the bottom and the air temperature at the top of the air preheater. In both figures, the parameters are the operating pressure and the air/gas flow rate. The maximum air/gas pressure is limited by the terminal velocity of the balls. At a too high velocity, the balls are blown out of the unit. The velocity of the balls and of the gas in the gas generator and in the air preheater is shown in Figs. 5 and 7. The balls initial velocity (at the top) is always zero and they reach their terminal velocity in a short distance. However, the terminal velocity changes along the way, because of variations in gas temperature. The gas and ball temperature variations

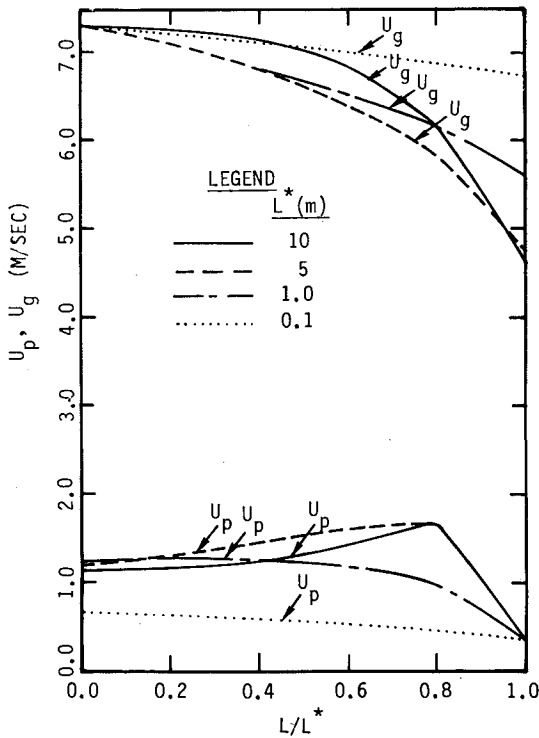


Fig. 5 Gas velocity and particle velocity in gas generator: stainless steel balls,  $d_p = 1.6$  mm,  $P = 30$  atm,  $\dot{m}/A = 43.95$  kg/m<sup>2</sup>·s.

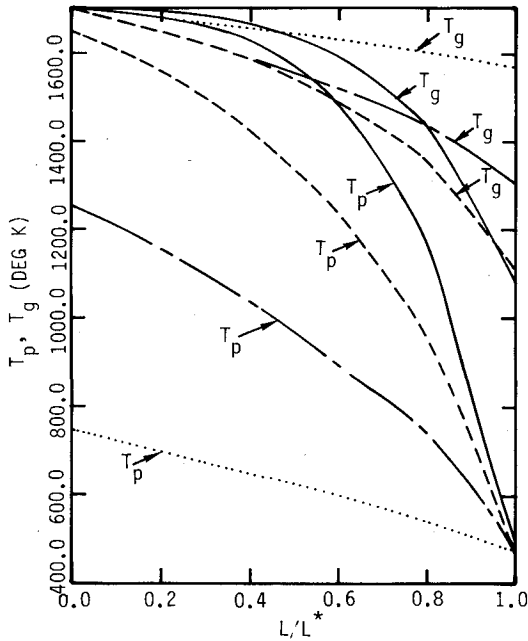


Fig. 6 Gas temperature and particle temperature in gas generator: stainless steel balls,  $d_p = 1.6$  mm,  $P = 30$  atm,  $\dot{m}/A = 43.95$  kg/m<sup>2</sup>·s (legend as in Fig. 5).

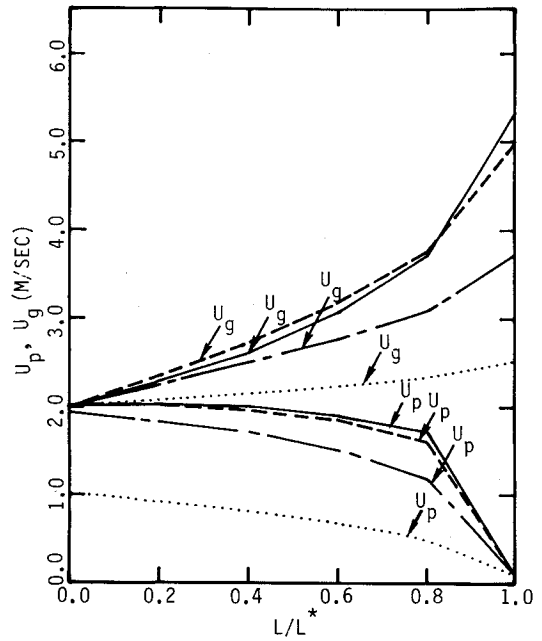


Fig. 7 Gas velocity and particle velocity in air preheater: stainless steel balls,  $d_p = 1.6$  mm,  $P = 30$  atm,  $\dot{m}/A = 53.43$  kg/m<sup>2</sup>·s (legend as in Fig. 5).

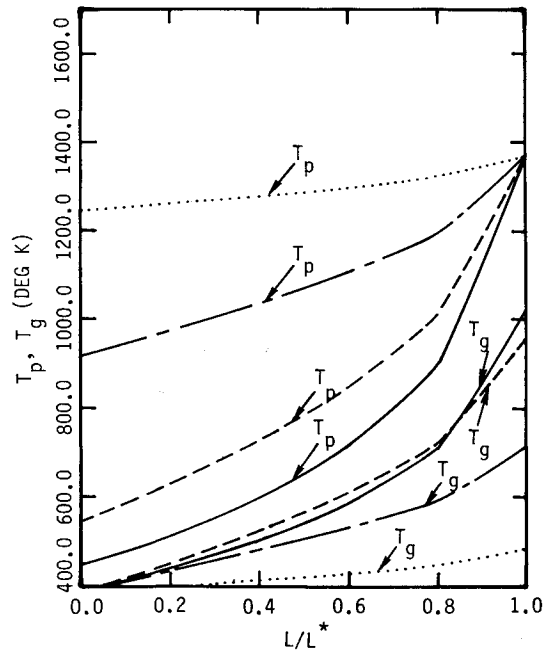


Fig. 8 Gas temperature and particle temperature in air preheater: stainless steel balls,  $d_p = 1.6$  mm,  $P = 30$  atm,  $\dot{m}/A = 53.43$  kg/m<sup>2</sup>·s (legend as in Fig. 5).

Table 6 Equations of motion in a convenient form for numerical integration

$$U'_p = -\frac{1}{U_g FR} + A \frac{C_D}{S} \quad (22)$$

$$U'_g = \left[ \left( 6S_t k_g \left( \frac{C_{pgi}^*}{R^*} \right) \frac{D}{S} \eta - Q \right) C + A \eta \frac{C_D}{S} E \right] / \Delta \quad (23)$$

$$T'_g = \left[ -A \eta \frac{C_D}{S} F - \left( 6S_t \frac{D}{A} k_g \left( \frac{C_{pgi}^*}{R^*} \right) \eta - Q \right) B \right] / \Delta \quad (24)$$

$$T'_p = 6S_t C_{pr} D \frac{k_g}{S} \quad (25)$$

where

$$\Delta = CF - BE \quad (26)$$

are shown in Figs. 6 and 8 for the gas generator and air preheater, respectively. Based on these calculations, the heat exchanger in Fig. 2 was sized to meet the plant requirements.

### Conclusions

1) A heat exchanger based on the CIBEX concept is smaller in size than a comparably rated conventional heat exchanger.

2) The computer code can be exercised to size and to design both units of the heat exchanger—the gas generator and the air preheater. Some features that the code indicates are:

a) Small balls are preferable to large ones, since they have a larger surface area per unit weight and a longer residence time (smaller terminal velocity). But too small balls limit the gas-phase mass flux (blow off of small balls by too high a gas velocity) and therefore an optimal ball size exists for each application.

b) Increased operating pressure reduces the overall size of the heat exchanger.

c) On a unit mass basis, ceramic balls are more effective than stainless steel balls. However, the durability of ceramic may not be as good as that of the stainless balls.

3) The CIBEX concept is uniquely capable of recovering very high level heat from effluent gases that may contain very reactive gas species such as  $H_2S$ ,  $COS$ ,  $CO$ , etc. In this case, ceramic balls are the preferred heat transfer material.

### Acknowledgment

The author wishes to thank the following individuals at TRW who sponsored and guided the work: A. P. Grossman, L. Manson, and H. L. Burge.

### References

- <sup>1</sup>Heywood J. B., and Womack G. J., (Eds.), *Open Cycle MHD Power Generation*, Pergamon Press, New York, 1969, pp. 194-212.
- <sup>2</sup>"Method for Effecting Chemical Reactions Between Cascading Solids and Counterflowing Gases or Fluids," patent held by Robert, H. Essenhigh, Scientific Research Instruments Corp., U.S. Patent 3,801,469, April 1974.
- <sup>3</sup>Yoon, S. M. and Kunii, D., "Gas Flow and Pressure Drop Through Moving Beds," *Industrial and Engineering Chemistry, Process Design and Development*, Vol. 9, No. 4, 1970, pp. 559-565.
- <sup>4</sup>Marble, F. E., "Dynamics of Dusty Gases," *Annual Review of Fluid Mechanics*, Vol. 2, 1970, pp. 397-446.
- <sup>5</sup>Baumeister, T., *Mark's Standard Handbook for Mechanical Engineers*, 7th ed., McGraw-Hill, New York, 1967.
- <sup>6</sup>Svehla, R. A., "Estimated Viscosities and Thermal Conductivities of Gases at High Temperatures," NASA TR R-132, 1962.
- <sup>7</sup>Hussein, M. F., "The Dynamic Characteristics of Solid Particles in Particulate Flow in Rotating Machinery," Ph.D. Thesis, University of Cincinnati, Ohio, 1972.
- <sup>8</sup>Lapple, C. E. and Shepherd, C. B., "Calculation of Particle Trajectories," *Industrial and Engineering Chemistry*, Vol. 32, No. 5, 1940, pp. 605-617. (See also Dring, R. P. and Suo, M., "Particle Trajectories in Swirling Flows," *Journal of Energy*, Vol. 2, No. 4, 1978, pp. 232-237).

*From the AIAA Progress in Astronautics and Aeronautics Series . . .*

## AEROTHERMODYNAMICS AND PLANETARY ENTRY—v. 77

## HEAT TRANSFER AND THERMAL CONTROL—v. 78

*Edited by A. L. Crosbie, University of Missouri-Rolla*

The success of a flight into space rests on the success of the vehicle designer in maintaining a proper degree of thermal balance within the vehicle or thermal protection of the outer structure of the vehicle, as it encounters various remote and hostile environments. This thermal requirement applies to Earth-satellites, planetary spacecraft, entry vehicles, rocket nose cones, and in a very spectacular way, to the U.S. Space Shuttle, with its thermal protection system of tens of thousands of tiles fastened to its vulnerable external surfaces. Although the relevant technology might simply be called heat-transfer engineering, the advanced (and still advancing) character of the problems that have to be solved and the consequent need to resort to basic physics and basic fluid mechanics have prompted the practitioners of the field to call it thermophysics. It is the expectation of the editors and the authors of these volumes that the various sections therefore will be of interest to physicists, materials specialists, fluid dynamicists, and spacecraft engineers, as well as to heat-transfer engineers. Volume 77 is devoted to three main topics, Aerothermodynamics, Thermal Protection, and Planetary Entry. Volume 78 is devoted to Radiation Heat Transfer, Conduction Heat Transfer, Heat Pipes, and Thermal Control. In a broad sense, the former volume deals with the external situation between the spacecraft and its environment, whereas the latter volume deals mainly with the thermal processes occurring within the spacecraft that affect its temperature distribution. Both volumes bring forth new information and new theoretical treatments not previously published in book or journal literature.

*Published in 1981, Volume 77—444 pp., 6×9, illus., \$35.00 Mem., \$55.00 List  
Volume 78—538 pp., 6×9, illus., \$35.00 Mem., \$55.00 List*

TO ORDER WRITE: Publications Dept., AIAA, 1633 Broadway, New York, N.Y. 10019